*J. Am. Chem. Soc.* **1982**, *104*, 4515-4520

# Configuration Interaction Study of the Three Lowest Electronic States in the $HCO_2$ and $CH_3CO_2$ Radicals

**Sigrid D. Peyerimhoff,**[*,†] **Philip S. Skell,**[*,‡] **Donald D. May,**[‡] **and Robert J. Buenker**[§]

*Contribution from the Lehrstuhl für Theoretische Chemie, Universität Bonn, D-5300 Bonn 1, West Germany, Department of Chemistry, The Pennsylvania State University, University Park, Pennsylvania 16802, and Lehrstuhl für Theoretische Chemie, Universität-Gesamthochschule Wuppertal, D-5600 Wuppertal 1, West Germany.* *Received November 11, 1981*

**Abstract:** The three lowest lying electrontic states of the formyl $HCO_2$ ($^2A_2$, $^2B_2$, and $^2A_1$) and the acetyl $CH_3CO_2$ ($1^2A''$, $^2A'$, $2^2A''$) radicals have been studied by multireference double-excitation configuration interaction calculations. Double-$\zeta$ basis sets including d functions are employed thereby. The core of doubly occupied MO's is chosen such that in each case 17 electrons can be distributed among the valence-shell orbitals, which leads to configuration spaces of order up to 1.06 million. All three states show potential minima within an energy range of ca.10 kcal/mol from one another and are primarily distinguished on the basis of their different behavior with respect to OCO angle variations. The fully symmetric $^2A'$ state in $CH_3CO_2$, which prefers large OCO angles, exhibits a very shallow CC stretch potential well, so that $CO_2$ loss is energetically quite likely in this state. In spite of the formal difference in nuclear symmetry there exists a close analogy between corresponding states in the two molecules, so that the present results also seem to be transferable to still larger carboxylic systems. All calculated results are compared with the most recent experimental observations on $\pi$- and $\sigma$-acetoxy radicals and very good agreement is found.

## 1. Introduction

In recent years there has been increased interest in radicals with low-lying electronic states, especially since it has been realized that such species can be produced in chemical reactions not only in the ground but also in some of their excited states.[1,2] This feature is of special importance since the radicals often times show a very different behavior in $\sigma$ than in $\pi$ states, even though the energy of the states might only differ by a few kilocalories/mole.

Among the simplest of such radicals are $HCO_2$ and $CH_3CO_2$, whereby the first can be characterized by relatively high ($C_{2v}$) symmetry, while the other belongs to only the $C_s$ group. It appears that only semiempirical treatments or SCF calculations (with at most a very limited CI) have thus far been employed[3] to investigate these radicals from the theoretical point of view. Since it is well known that single-determinantal wave functions are generally not capable of giving reliable energy differences between various electronic states, it is the goal of the present contribution to study the stability and electronic structure of these two radicals by employing large-scale configuration interaction calculations, which treatment has proven to be very successful over the last years in predicting molecular stabilities in electronic states of arbitrary characteristics and/or geometrical conformations.[4] At the same time direct comparison with experimental results will be made.

## 2. Theoretical Treatment

The coordinate system employed for each radical is given in Figure 1. The $CO_2$ group is thereby taken to be symmetric and to lie in the *xy* plane in each case. The $CH_3$ group is chosen such that a plane of symmetry is maintained in the $CH_3CO_2$ system; i.e., one of the CH bonds is located in the *xz* plane bisecting the OCO angle. No other orientation of the $CH_3$ group relative to the $CO_2$ fragment is considered in what follows.

In $HCO_2$ three geometrical variables, CO and CH distances and angle OCO, have been optimized explicitly for the three low-lying electronic states under the assumption of a symmetrical structure. For $CH_3CO_2$ the optimum CO bond lengths of $HCO_2$ have been employed without further optimizaion, and a standard $CH_3$ conformation (CH = 1.085 Å, and <HCH = 109.5°) has also been used, so that the only geometrical variables in the acetyl radical which remain subject to change in the present investigation are the C–C bond lengths and the $CO_2$ angle. The latter quantity appears to be the most critical variable since it is well known from previous work[5,6] on $HCOO^-$ or $O_3$ that the angular characteristics are quite different for the various low-energy states in such systems.[7,8]

The AO basis set employed is of double-$\zeta$ quality augmented by a d functions on each of the heavy atoms and some s-type bond functions to better account for polarization effects. The main portion of the basis is taken from the work of Dunning[9] in the (6, 1, 1, 1|4, 1) contraction for the oxygen and carbon atoms; the d-function exponent for oxygen is chosen to be $\alpha = 1.33$, while for carbon it is $\alpha = 0.64$. The s bond function located at the center of each of the CO bonds has an exponent of $\alpha = 1.3$, in accordance with prior work.

For $HCO_2$ a slightly more flexible description of the sole hydrogen is employed than for the $CH_3$ group in the larger system: two s functions in a (4,1) contraction are located at the hydrogen nucleus, in addition to a H–C bond s species ($\alpha = 1.3$), while in $CH_3CO_2$ only a five-component expansion (with scaling factor $\eta^2 = 2.0$) is taken for each of the three hydrogens. Thus the calculation for $HCO_2$ comprises a total of 53 AO's, although a few calculations are also carried out without the extra d polarization species in order to estimate their importance (35 functions in all). The total AO basis of $CH_3CO_2$ consists of 70 contracted Gaussians, including an s function with exponent $\alpha = 1.0$ placed in the center of the CC bond.

The CI calculations are of the standard multireference single- and double-excitation (MRD-CI) type with configuration selection and energy extrapolation, as described elsewhere.[10] In the present treatment for $HCO_2$ a core of three shells is maintained doubly occupied in all configurations, corresponding to the K shells in

---

† Universität Bonn.
‡ The Pennsylvania State University.
§ Universität-Gesamthochschule Wuppertal.

(1) (a) P. S. Skell and J. C. Day, *Acc. Chem. Res.*, **11**, 381 (1978), and references therein; (b) J. P. Slanga, J. C. Day, and P. S. Skell, *Angew. Chem., Int. Ed. Engl.*, **17**, 515; (1978) (c) P. S. Skell and J. C. Day, *J. Am. Chem. Soc.* **100**, 1951 (1978); (d) R. L. Tlumak and P. S. Skell, *ibid* in press.

(2) P. S. Skell and D. D. May, *J. Am. Chem. Soc.*, **103** 967 (1981).

(3) (a) N. C. Baird and K. F. Taylor, *Can. J. Chem.*, **58** 733 (1980); (b) T. Koenig, R. A. Wielesek, and J. G. Huntington, *Tetrahedron Lett.*, 2283 (1974); (c) O. Kikuchi, *ibid.* 2421 (1977); (d) O. Kikuchi, A. Hiyama, H. Yoshida, and K. Suzuki, *Bull. Chem. Soc. Jpn.* **51**, 11 (1978); (e) J.M. McBride and R.A. Merrill, *J. Am. Chem. Soc.*, *102*, 1723 (1980).

(4) See, for example; S.D. Peyerimhoff and R.J. Buenker in "Computational Methods in Chemistry", J. Bargon, Ed., Plenum Press, New York, p (1980) 175.

(5) S. D. Peyerimhoff, *J. Chem. Phys.* **47**, 349 (1967).

(6) S. D. Peyerimhoff and R. J. Buenker, *J. Chem. Phys.*, **47**, 1953 (1967).

(7) A.D. Walsh, *J. Chem. Soc.*, 2260 (1953), and following articles.

(8) R.J. Buenker and S.D. Peyerimhoff, *Chem. Rev.*, **74**, 127 (1974).

(9) Th. Dunning, *J. Chem. Phys.* **53**, 2823 (1970).

(10) (a) R. J. Buenker and S.D. Peyerimhoff, *Theor. Chim. Acta*, **35**, 33 (1974); **39**, 217 (1975); (b) R.J. Buenker, S.D. Peyerimhoff, and W. Butscher, *Mol. Phys.*, **35**, 771 (1978); (c) R. J. Buenker in "Molecular Physics and Quantum Chemistry into the '80's", P.G. Burton, Ed., University of Wollongong Press, 1980, pp 1.5.1–1.5.40.

0002-7863/82/1504-4515$01.25/0

Table I. Technical Details of the CI Calculations for the First Three Electronic States in $HCO_2$

| state | reference set (occupation) | | | | | | | | | | CI space generated/ selected (av) |
|---|---|---|---|---|---|---|---|---|---|---|---|
| | $3a_1$ | $4a_1$ | $5a_1$ | $6a_1$ | $2b_2$ | $3b_2$ | $4b_2$ | $1a_2$ | $1b_1$ | $2b_1$ | |
| $^2A_1$ | ...2 | 2 | 2 | 1 | 2 | 2 | 2 | 2 | 2 | | 306 666/8400-8800 |
| | ...2 | 2 | 2 | 1 | 2 | 2 | 2 | 2 | | 2 | |
| | ...2 | 2 | 2 | 1 | 2 | 2 | 2 | | 2 | 2 | |
| | ...2 | 2 | 2 | 1 | 2 | 2 | 2 | 2 | 1 | 1 | |
| | ...2 | 2 | 2 | 2 | 2 | 1 | 2 | 1 | 2 | 1 | |
| | ...2 | 2 | 2 | 2 | 2 | 2 | 1 | 1 | 2 | 1 | |
| $^2B_2$ | ...2 | 2 | 2 | 2 | 2 | 2 | 1 | 2 | 2 | | 277 675/8370-8760 |
| | ...2 | 2 | 2 | 2 | 2 | 2 | 1 | 2 | | 2 | |
| | ...2 | 2 | 2 | 2 | 2 | 2 | 1 | 2 | 1 | 1 | |
| | ...2 | 2 | 1 | 2 | 2 | 2 | 2 | 1 | 2 | 1 | |
| | ...2 | 2 | 2 | 1 | 2 | 2 | 2 | 1 | 2 | 1 | |
| $^2A_2$ | ...2 | 2 | 2 | 2 | 2 | 2 | 2 | 1 | 2 | | 221 993/8350-8820 |
| | ...2 | 2 | 2 | 2 | 2 | 2 | 2 | 1 | | 2 | |
| | ...2 | 2 | 2 | 2 | 2 | 2 | 2 | 1 | 1 | 1 | |
| | ...2 | 2 | 2 | 2 | 2 | 2 | 2 | 1 | 1 | ($4b_1$) | |

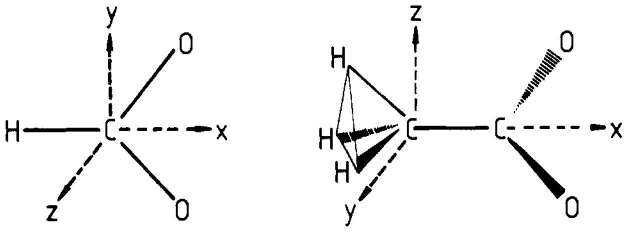

**Figure 1.** Coordinate system employed for the present treatment of $HCO_2$ and $CH_3CO_2$.

carbon and oxygen, respectively. The three highest virtual MO's are discarded entirely, so that a total of 17 electrons is distributed by the CI procedure in $HCO_2$ among 47 orbitals. Comparison with $HCO_2^-$ and $O_3$, which possesses the ground-state electronic configuration $...6a_1^2 1a_2^2 4b_2^2$, suggests three low-energy states in $HCO_2$ which result by removing one electron from one of the three highest occupied orbitals, which are almost isoenergetic in $O_3$, for example. The symmetries of these states are thus $^2B_2$, $^2A_2$, and $^2A_1$, with the $6a_1$ classified as symmetric, the $b_2$ as an antisymmetric orbital in the OCO plane, and the $a_2$ as a $\pi^*$-type species; the calculated charge density contours for the two $\sigma$-type MO's are given in Figure 2.

Separate SCF calculations have been undertaken for each state of $HCO_2$ and the resulting SCF-MO's have then been employed as the one-electron basis for the corresponding CI calculations, which have been carried out for a total of 22 geometrical conformations. The reference set for the CI treatment comprises all configurations with a contribution of more than 0.2% to the final wave-function expansion, which amounts to six configurations in the $^2A_1$ case, four for $^2A_2$, and five such species for the $^2B_2$ state; details of the reference sets are listed in Table I. The selection threshold was set to $T = 10$ $\mu$hartree, so that out of approximately 300 000 generated configurations (see Table I), between 8300 and 8800 are treated directly in the secular equations. The CI spaces for the basis containing only 35 AO's are naturally much smaller, namely, 87 946 for $^2A_1$ (4500–4800 selected), 65 061 for $^2A_2$ (4430–4640 selected), and 87 809 for $^2B_2$ (4530–4650 selected). In addition to the extrapolated energy $E$(MRD-CI), which corresponds to the number of configurations which have been generated, the energy which would result from a full CI in the AO basis employed is also estimated according to the formula[11,12]

$$E(\text{full CI est}) = E(\text{MRD-CI}) + [E_{\text{ref}} - E(\text{MRD-CI})](1 - \textstyle\sum^{\text{ref}} c_0^2)$$

with the sum taken over all configurations in the reference set.

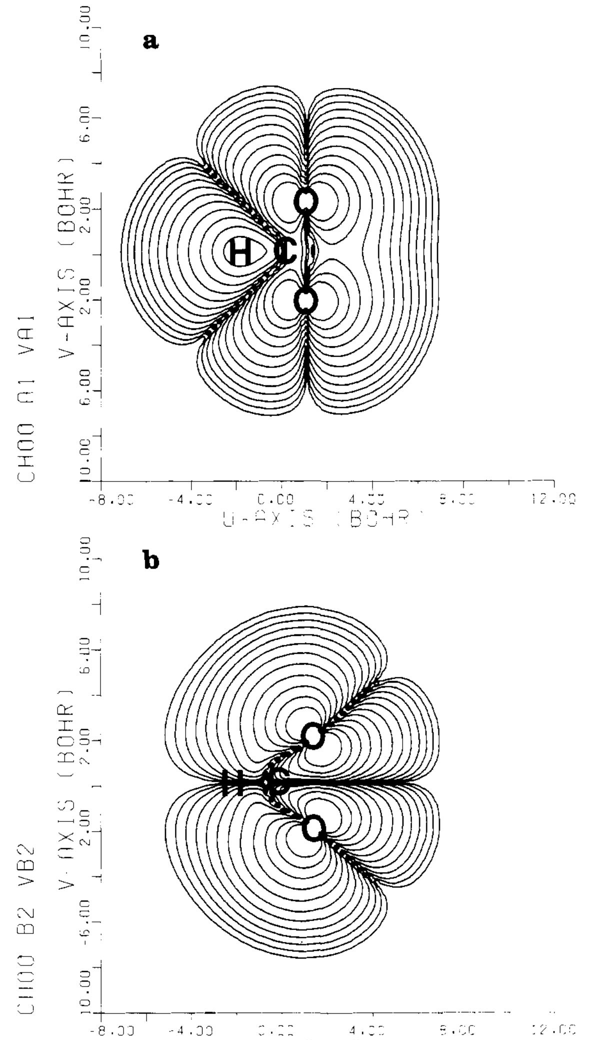

**Figure 2.** Calculated charge density contours of the singly occupied orbital $6a_1$ ($\sigma_S$) and $4b_2$ ($\sigma_A$) in the $^2A_1$ and $^2B_2$ radicals, respectively; the optimum $C_{2v}$ geometry is employed in each case.

Essentially equivalent MRD-CI calculations are carried out for the $CH_3CO_2$ system. Because of the lower nuclear symmetry two of the states in $HCO_2$, namely, $^2A_2$ and $^2B_2$, are found in the same irreducible representation (A″) in this case, while $^2A_1$ transforms as A′ in this point group. The lower symmetry together with the fact that there are more valence electrons in this system leads to much larger secular equations than are encountered in $HCO_2$; it was therefore decided to leave seven MO's doubly

---

[11] S.R. Langhoff and E.R. Davidson, Int. *J. Quantum Chem.* **8**, 61 (1974).

[12] P.J. Bruna, S.D. Peyerimhoff, and R.J. Buenker, *Chem. Phys. Lett.*, **72**, 278 (1980).

Table II. Technical Details of the CI Calculations for the First $^2A'$ and the Two Lowest $^2A''$ States in $CH_3CO_2$

| state | reference set[a] (occupation) | | | | | | | | | | treatment[b] | CI space generated/ selected |
|---|---|---|---|---|---|---|---|---|---|---|---|---|
| | 6a | 7a | 8a | 9a | 10a | 11a | 3b | 4b | 5b | 6b | | |
| $^2A_1$ | ...2 | 2 | 2 | 2 | 1 | | 2 | 2 | 2 | 2 | 1M1R | 109 092/9650-9890 |
| | ...2 | 2 | 2 | 2 | 1 | 2 | 2 | 2 | | 2 | 2M1R | 378 974/9310-9710 |
| | ...2 | 2 | 1 | 2 | 1 | 1 | 2 | 2 | 2 | 2 | 6M1R | 1 066 664/9090-9470 |
| | ...2 | 2 | 2 | 1 | 1 | 1 | 2 | 2 | 2 | 2 | | |
| | ...2 | 2 | 2 | 2 | 2 | 1 | 1 | 2 | 1 | 2 | | |
| | ...2 | 2 | 2 | 2 | 2 | 1 | 2 | 2 | 1 | 1 | | |
| $^2A''$ | ...2 | 2 | 2 | 2 | 2 | | 2 | 2 | 2 | 1 | 3M2R | 255 257/8500-8900 |
| | ...2 | 2 | 2 | 2 | 2 | | 2 | 1 | 2 | 2 | 4M2R | 499 656/8000-8300 |
| | ...2 | 2 | 2 | 2 | 2 | | 2 | 2 | 1 | 2 | 5M2R | 683 416/6900-9360 |
| | ...2 | 1 | 2 | 2 | 2 | 1 | 2 | 2 | 1 | 2 | 6M2R | 815 511/7000-9300 |
| | ...2 | 2 | 2 | 1 | 2 | 1 | 2 | 2 | 1 | 2 | 7M2R | 999 007/6600-8500 |
| | ...2 | 2 | 2 | 2 | 1 | 1 | 2 | 2 | 1 | 2 | | |
| | ...2 | 2 | 2 | 2 | 1 | 1 | 2 | 2 | 2 | 1 | | |

[a] The configurations are given in order of their importance. [b] $xMyR$ denotes $x$ reference (main) configurations and $y$ roots for which selection has been carried out.

occupied throughout (core = 7), i.e., three more than would results from the K shells alone. Thus in this treatment there also remain 17 electrons to be distributed among the various valence MO's in the CI, of which there are 59 in the present case (the three highest lying virtual orbitals are again discarded). Nevertheless it is seen from Table II, which lists some technical details, that the number of generated configurations is over a million in this case (the notation $xMyR$ in the table indicates that the generated space is obtained by taking all single and double excitations with respect to $x$ references species, while the selection procedure is carried out with respect to the lowest $y$ roots of the corresponding reference secular equation). In order to test convergence properties, several treatments with differing numbers of reference configurations are carried out; in addition SCF-MO's of the $^2A'$ as well as for the lowest $^2A''$ state are employed in various instances for the calculation of the two $^2A''$ roots in order to further evaluate the reliability of the results. The selection threshold for the $^2A'$ space is always $T = 10$ μhartree, while it is varied between $T = 15$ and 20 μhartree for the A″ configurations in order to keep the final configuration set to be explicitly diagonalized under order 10 000. At such thresholds the extrapolated ($T = 0$) CI energy values are on the average 0.08 ($HCO_2$) and 0.13 ($CH_3CO_2$) hartree lower than the corresponding secular equation eigenvalues obtained by explicit diagonalization.

## 3. Results for $HCO_2$

From simple molecular orbital theory as applied to $O_3$ and $HCO_2^-$,[5,6] it is expected that the three states $^2A_1$, $^2B_2$, and $^2A_2$ have quite different angular characteristics and hence this degree of freedom has been investigated first. A standard CH bond length of 1.085 Å ($2.05a_0$) and a CO bond distance of 1.25 Å ($2.362a_0$) is chosen in accordance with known equilibrium bond separations in $HCO_2^-$ and HCOOH. The calculated angular potential curves obtained at different levels of treatment are collected in Figure 3 a–c.

As expected from the qualitative theory[7,8] and the nodal structure of the various key orbitals (Figure 2), the $^2B_2$ state, in which the strongly O–O antibonding $4b_2$ orbital is only singly occupied, exhibits the smallest equilibrium bond angle, while the $^2A_1$ state, in which the $6a_1$ with its opposite angular behavior is only singly occupied, shows a minimum at a quite large angle. This qualitative trend is present at all three levels of treatment: SCF, MRD-CI, and estimated full CI.

If the configuration interaction results are compared with those of the optimal single configurations, the most prominent feature is the change in relative energy of the $^2A_2$ (π-type) state; the relative location of the two σ-type states, $^2A_1$ and $^2B_2$, is thereby much less affected by the CI (their spacing at 110°, for example, is reduced from 2.06 eV in the SCF treatment to 1.63 eV in the CI). On an absolute scale the present CI calculations simply show that the $^2A_1$ state of $HCO_2$ possesses the greatest correlation energy error and thus its energy lowering due to configuration mixing is largest, while the CI lowering for the $^2A_2$ state is the least of the three states under discussion. As a result the $^2B_2$ state becomes the lowest state of the three after CI and while in the SCF treatment the competition would appear to be between the $^2A_2$ (π) and $^2B_2$ (antisymmetric σ), the more realistic treatment

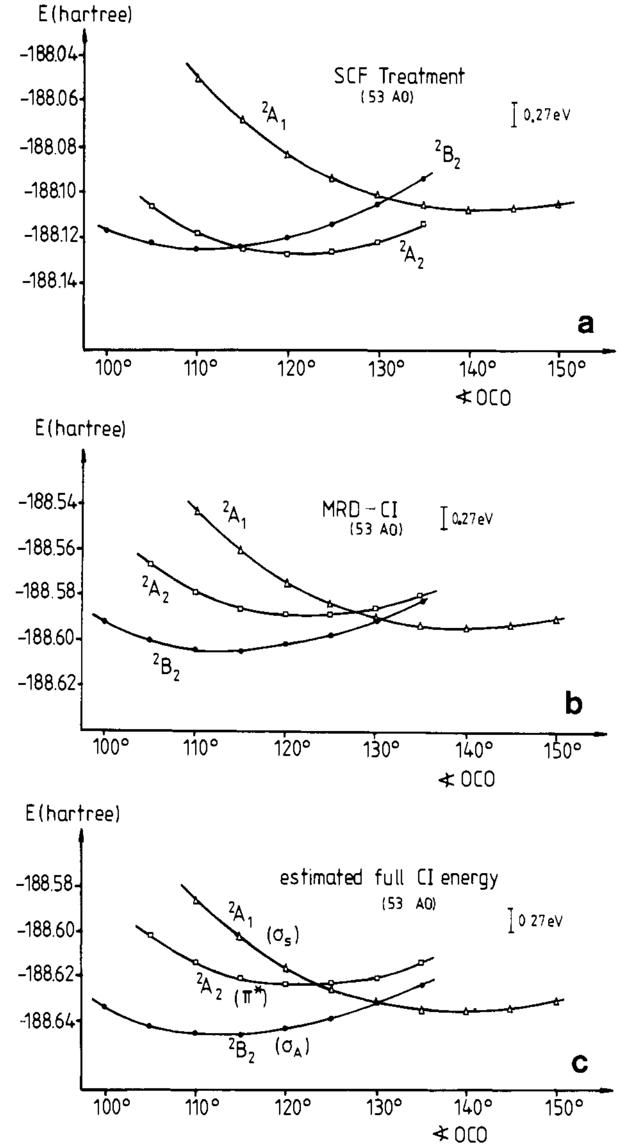

**Figure 3.** Calculated potential energy curves as a function of angle OCO for three states of $HCO_2$ at three levels of treatment: (a) SCF, (b) MRD-CI, and (c) estimated full CI limit. The basis set consists of 53 AO's (CH = 2.050 au., CO = 2.362 au).

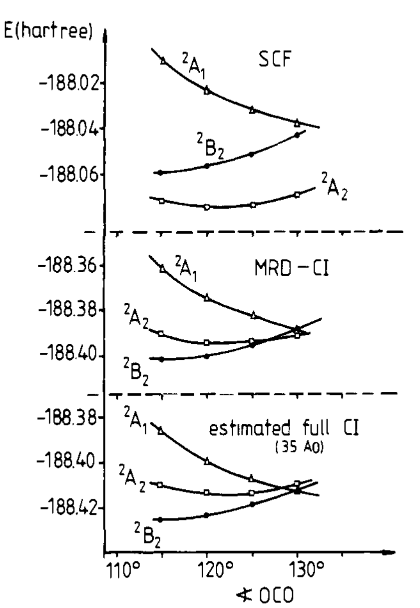

**Figure 4.** Calculated potential energy curves as a function of angle OCO for three states of $HCO_2$ at three levels of treatment as in Figure 3 but with the smaller AO basis set of 35 AO's without d functions.

shows all three states to lie in the same immediate neighborhood, especially between 120 and 130°.

Similar behavior is also apparent in the smaller AO basis calculations without d functions (Figure 4). The insufficient representation of the $a_2$ MO (which makes use of d orbital participation) leads to a situation in which the states which doubly occupy this species ($^2B_2$ and $^2A_1$) show higher energies relative to the $^2A_2$, which only singly occupies this orbital. The effect of this AO basis deficiency is considerably larger in the SCF calculations (Figure 3a and top of Figure 4) than at the estimated full CI level of treatment (Figure 3c and bottom of Figure 4), however. From this investigation it is clear that d AO's are important in representing the proper charge distribution in this molecule and hence only basis sets including d functions are dealt with in what follows.

Further minor changes are found in varying the other two structural parameters, CO bond length and CH separation. A three-point interpolation of the CH distance leads essentially to the same value as had been chosen originally, and hence no further optimization was undertaken for this geometry. The various optimum values for the other structural data are summarized in Table III, together with the corresponding energies. It is seen that the minimum-to-minimum energy splitting between the states is only in the order of 7 kcal/mol; this quantity is obtained without taking into account any zero-point energy corrections, or possible vibrational excitations resulting from a given reaction process, however. The computed vertical transition energies relative to the $^2B_2$ state in its equilibrium conformation are 16.6 ($^2A_2$) and 31.1 ($^2A_1$) kcal/mol, respectively. These values are in reasonably good agreement with published estimates[3c] for the corresponding quantities based on experiments for the related benzoyloxyl radical (13 and either 55 or 25 kcal/mol).

Asymmetric geometries, i.e., with unequal CO bond lengths, are not favored for the $\pi$-type radical. Explicit calculations have been carried out at the $^2A_2$ optimum geometry for $\Delta CO = \pm 0.06$ and $\pm 0.12$ au, at which points the total CI energy is found to be higher by 2 and 4 kcal, respectively. These calculations have been undertaken in a 6M2R treatment in order to also obtain an estimate for the location of the second $^2A''$ ($^2B_1$) electronic state, found to lie 78 kcal above the $^2A_2$ at this geometry (122°, 2.41 au) with a considerably steeper slope, i.e., an energy increase of 4.2 and 13 kcal for the corresponding asymmetric variations. It should also be noted that the CI energy difference for the $^2A_2$ state at the high-symmetry point was only 0.0005 hartree between the original 4M1R tratment employing $C_{2v}$-symmetry SCF orbitals and the 6M2R treatment employing a basis of $C_s$-symmetry SCF MO's. By contrast, the SCF energy changes from -188.12308 in the $C_{2v}$ to −188.1316 hartree in the $C_s$ point group calculations owing to symmetry breaking.

Table III. Optimal Geometrical Data for the Various States of $HCO_2$ under Discussion and Corresponding Energies[a]

| state | ∠OCO (deg) | CO dist (au) | $E$(MRD-CI) (hartree) | $E$(est full CI) (hartree) |
|---|---|---|---|---|
| $^2B_2$ | 113 | 2.39 (1.265 Å) | −118.605 53 | −118.6475 |
| $^2A_1$ | 139 | 2.36 (1.249 Å) | −118.593 87 | −118.6360 |
| $^2A_2$ | 122 | 2.41 (1.275 Å) | −118.589 52 | −118.6256 |
| state | | relative energies (eV) | | |
| $^2B_2$ | | 0.0 | | 0.0 |
| $^2A_1$ | | 0.317 (7.3 kcal) | | 0.312 (7.2 kcal) |
| $^2A_2$ | | 0.436 (10 kcal) | | 0.595 (13.7 kcal) |

[a] The CH bond length is chosen to be 2.05 au (1.085 Å) for all three states which is very close to the optimum value according to the calculations; the CO bonds are assumed to be equal (see also text).

The situation is somewhate different for the two energetically neighboring states, $^2B_2$ and $^2A_1$, since in this case an asymmetric distortion of the $CO_2$ framework leads to a Jahn–Teller (vibronic) mixing of both states, formally referred to as $1^2A'$ and $2^2A'$ in the lower order point group. A small decrease in energy upon asymmetric CO stretch is observed near the crossing point in the lower state, which is reduced to approximately 1 kcal further away from the crossing point ($\Delta CO \pm 0.06$ au from the $^2B_2$ minimum), while a comparable increase in energy is observed for the other asymmetric ($\Delta CO = \pm 0.12$ au) structure calculated for the upper $^2A'$ species. In this case the CI expansion must be quite extensive in order to overcome the effect of the symmetry breaking of the two $\sigma$ states at the SCF level of treatment. From an experimental point of view a relatively easy transition from the $^2B_2$ to $^2A_1$ potential curves can be expected in this area of mixed vibronic levels as a result of the asymmetric CO stretching motion.

## 4. Results for $CH_3CO_2$

The main distinction in this system compared to $HCO_2$ is the fact that because of the lower symmetry introduced by the methyl group the $^2A_2$- and $^2B_2$-type states (both antisymmetric with respect to the $xz$ plane perpendicular to the OCO plane; see Figure 1) are both classified as $^2A''$ species and hence are free to mix with one another. They still retain their basic characteristics, however, as can be seen by comparing Figure 3a–c with the results for $CH_3CO_2$ presented in Figure 5a,b. Since the SCF solution has only been obtained for the lowest state of $^2A''$ symmetry, the second such species is absent in Figure 5a.

Since the scope of the $CH_3CO_2$ computations was considerably larger than for the formyl radical, for which all configurations with a contribution of more than 0.2% have been included in the reference set, a number of calculations with differing numbers of reference species has been undertaken in this instance. A typical example demonstrating the type of convergence obtained is presented in Table IV. The estimated full CI energy for the $^2A'$ state differs in all cases (10 different geometries) by less than 0.001 hartree among the treatments employing two and six reference configurations, respectively, whereby only six such species (just as in the $^2A_1$ calculation of $HCO_2$) appear to contribute more than 0.2% to the total wave function.

The situation for the two $^2A''$ states is somewhat more complicated since a total of 9, and in the mixing zone up to 11, configurations are found to exceed the 0.2% $c^2$ threshold. Since seven reference species already lead to approximately 1 000 000 configurations (Table II), another route for testing the convergence is taken in this case. Two different orbital bases are employed, namely, that of the $^2A''$ SCF solution as well as that resulting from the $^2A'$ SCF calculations. The results of Table IV again offer a typical example: the 7M2R ($^2A''$MO's) and the 6M2R ($^2A'$ MO's) treatments differ by 0.001–0.002 hartree for the first root (full CI estimate) and up to 0.005 hartree in the second root. From these various tests it would appear that the uncertainty in

Table IV. Typical Results for the $^2A'$ and $^2A''$ States of $CH_3CO_2$ (Geometry: ∠OCO = 120°, CC = 1.50 Å, CH = 1.085 Å, CO = 1.27 Å)

| treatment[a] | $\Sigma^{ref}c_0^2$ (%) | secular eq size | $E$(MRD-CI) | $E$(full CI est) |
|---|---|---|---|---|
| | | $^2A'$ State | | |
| 1M1R ($^2A'$ MO's) | 88.29 | 9650 | −227.5404 | −227.5882 |
| 2M1R ($^2A'$ MO's) | 89.75 | 9313 | −227.561 50 | −227.6015 |
| 6M1R ($^2A'$ MO's) | 90.67 | 9071 | −227.566 48 | −227.6022 |
| | | all $T$ = 10 μhartree | | |
| | | $1^2A''$ State | | |
| 3M2R ($^2A''$ MO's) | 88.73 | 9259 | −227.578 38 | −227.6242 |
| 4M2R ($^2A''$ MO's) | 89.50 | 6543 | −227.582 67 | −227.6254 |
| 7M2R ($^2A''$ MO's) | 91.25 | 6597 | −227.598 75 | −227.6331 |
| 3M2R ($^2A'$ MO's) | 89.03 | 6487 ($T$ = 30) | −227.574 96 | −227.6210 |
| 6M2R ($^2A'$ MO's) | 90.16 | 9285 | −227.591 73 | −227.6311 |
| | | all $T$ = 20 μhartree | | |
| | | $2^2A''$ State | | |
| 3M2R ($^2A''$ MO's) | 88.70 | same as for $1^2A''$ state | −227.564 30 | −227.6107 |
| 4M2R ($^2A''$ MO's) | 89.91 | | −227.566 48 | −227.6067 |
| 7M2R ($^2A''$ MO's) | 91.04 | | −227.577 31 | −227.6124 |
| 3M2R ($^2A'$ MO's) | 89.04 | | −227.559 5 | −227.6036 |
| 6M2R ($^2A'$ MO's) | 91.73 | | −227.577 7 | −227.6091 |

[a] For notation see footnote $b$ in Table II.

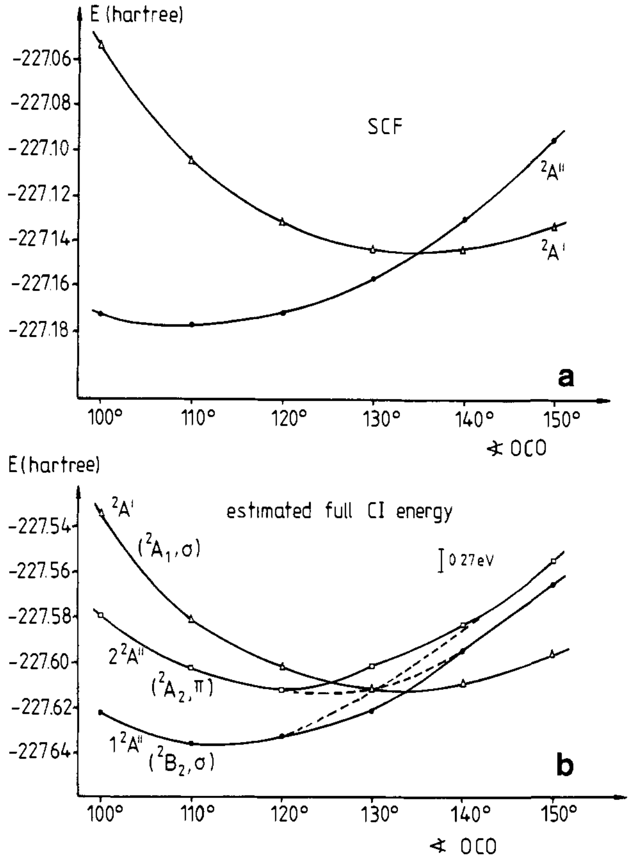

**Figure 5.** (a) Calculated SCF potential curves for the first two states of $^2A'$ and $^2A''$ symmetry in $CH_3CO_2$ as a function of the OCO angle (CH = 1.085 Å, <HCH = 109° 54′, CC = 1.50 Å, CO = 1.25 Å). (b) Calculated potential energy curves for the three lowest states in $CH_3CO_2$ as a function of the OCO angle; the estimated full CI is plotted. (other geometrical variables as in Figure 3a). The unperturbed states in the avoided crossing are indicated by dashed lines.

the CI result (within the given AO basis and doubly occupied core) is only in the order of approximately 0.03 eV for the $^2A'$ state, but it can be several times larger in the two $^2A''$ states, with the largest uncertainties expected to occur in the mixing zone; these data should certainly be kept in mind in evaluating the overall results.

Finally, the question of whether the number of electrons allowed variable occupation in the CI could be further reduced has been checked for a number of geometrical conformations by employing nine instead of seven doubly occupied shells in the core (i.e., 13 valence electrons only). This treatment results in essentially parallel potential curves, wherby the $^2A'$ energies (three points) are higher by 0.162–0.163 hartree, those of the $1^2A''$ state (seven points) by 0.151–0.153 hartree, and those of the $2^2A''$ state by 0.149–09151 hartree. In other words, the larger core provides a slightly worse representation of the $^2A_1$ state, thus leading to larger energy separations among those states than is encountered in the better treatment. This feature is consistent with what has already been found in $HCO_2$ in going from either SCF to CI or from the smaller AO basis to the larger more flexible representation.

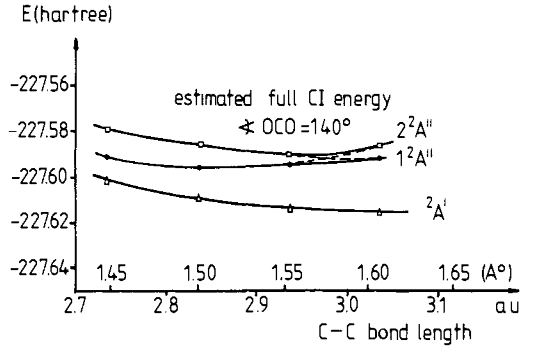

**Figure 6.** Calculated potential energy curves for the CC stretching mode in $CH_3CO_2$; the estimated full CI energy is plotted (CH and CO bond-lengths as in Figs. 4, OCO = 140°).

Finally, an important degree of freedom, namely, the C–C stretch vibration in $CH_3CO_2$, has also been investigated and the results of these calculations are presented in Figure 6. While both $^2A''$ states show a definite minimum, the $^2A'$ species exhibits an extremely flat CC stretch potential curve. It would thus seem that $CO_2$ cleavage in the $^2A'$ state can be achieved with considerable ease, especially since the wide-angle structure of this σ-type radical is also relatively close to the known linear geometry of the $CO_2$ molecule (see also Figure 2).

The approximate minima in the electronic energy surface of each state, taken under the assumption that the energy lowering at the respective optimum internuclear OCO angle due to C–C stretch is the same as that calculated at ∠OCO = 140° (Figure 6), and also by neglecting any energy differences between the radicals due to the slightly different CO bond lengths in the various states, are collected in Table V. The close analogy to the data for $HCO_2$ (Table III) is quite apparent. No special significance should be attached to the fact that both the $^2A'$ and $2^2A''$ minima seem to be very nearly isoenergetic, since the errors in the treatment, as pointed out earlier, are conceivably in the order of

Table V. Optimal Geometrical Data for the Various $CH_3CO_2$ States under Discussion and Corresponding Energies Estimated from the Calculated Curves of Figures 3 and 4

| state | OCO (deg) | CC (Å) | E(est full CI) (hartree) |
|---|---|---|---|
| $1^2A''$ | 112 | 1.5 | -227.6365 |
| $^2A'$ | 135 | 1.60 | -227.619 |
| $2^2A''$ | 122 | ≈1.57 | -227.619 |

| state | relative energies (eV) |
|---|---|
| $1^2A''$ | 0.0 |
| $^2A'$ | 0.476 (10.9 kcal) |
| $2^2A''$ | 0.476 (10.9 kcal) |

several kcal/mol, and are likely to place the $^2A'$ state somewhat too high compared with the $1^2A''$.

## 5. Observations on $RCO_2$ Behavior (PSS and DDM)

Experimental results which will be reported in detail elsewhere show a remarkable concordance with these calculations, perhaps a concordance which is unique at present, but which holds promise of a future in which theory and experiment will be intimate and specific companion methods for examination of chemical dynamics.

The two methods employed for generating $RCO_2$ radical (R = Me, Et, *i*-Pr, or *t*-Bu) are:

$$\text{method I:}\quad RCO_2Br + Br\cdot \rightarrow Br_2 + RCO_2$$

$$\text{method II:}\quad RCO_2Br + R'\cdot \rightarrow R'Br + RCO_2$$

These methods differ in that method II is more exothermic than I by an amount equal to the bond energy difference between $Br_2$ and R'Br, 21.7 kcal/mol if R' is a primary or secondary alkyl radical. If excited states lie within this energy gap, it is resonable to anticipate[1] that methods I and II will populate different $RCO_2$ states.

If studied in thermal chain reactions having I or II integral to the chain steps, both of these methods produce H-abstracting radicals showing selectivities for abstractions from primary or secondary C–H bonds with early transition state character. These selectivities are nonetheless different from one another and thus require two H abstractors. In competition with these H-abstraction reactions is the well-known loss of $CO_2$, leading to R· and ultimately RBr (the Hunsdiecker reaction).

These competition processes were discerned readily at temperatures between -63 and -100 °C. Remarkably, the loss of $CO_2$ (method I or II) occurs with higher activation energies than the H abstractions, accounting for the earlier failures to recognize chemistry other than the loss of $CO_2$, since those studies were carried out at room temperature or above. A second unexpected feature of these observations is that *t*-$BuCO_2$ decarboxylates less rapidly by a factor of 10 than $EtCO_2$, the difference in rate being caused by the ~1 kcal/mol larger $E_{act}$ for loss of $CO_2$ from the former radical.

These facts are neatly consistent with the rationalization provided by Figures 5 and 6. The decarboxylating $RCO_2$ is $^2A'$. Steric hindrance to opening the OCO angle from 120 to 140° places the potential energy curve for *t*-$BuCO_2$ higher than that for $EtCO_2$. By analogy with the earlier empirically based assignments,[1] the H abstractor of method I is the $2^2A''$, and the H abstractor of method II is the $1^2A'$.

## 6. Summary

In conclusion the present calculations point out the close analogy between the formyl and acetyl radicals despite their difference in nuclear symmetry. It is expected that this analogy can also be carried over to still large carboxylate radicals. The calculations show three low-lying electronic states in these systems whose potential energy minima are separated by probably less than 10 kcal; consideration of vibrational effects might easily reduce this energy gap further. The states show different characteristics with respect to OCO angle variation with the fully symmetric state preferring the large-angle structure (135–140°). In $CH_3CO_2$ this state is also characterized by a very shallow CC potential well, which should favor $CO_2$ cleavage; both $^2A''$ states exhibit a deeper CC potential minimum. These calculations are in full accord with the experimental observations in low-temperature radical chain reactions which recognize from kinetic evidence $RCO_2$'s which have two low-lying H-abstracting states, each of which has an energy barrier to loss of $CO_2$.

**Acknowledgment.** The services and computer time made available by the University of Bonn Computer Center (RHRZ) have been essential to this study and are gratefully acknowledged. The kinetic evidence was obtained at The Pennsylvania State University in a research program supported by the National Science Foundation (CHE-7810049).

Registry No. $HCO_2$, 16499-21-1; $CH_3CO_2$, 13799-69-4.

---

# Electron-Exchange Processes by Organic Solids: An Electrochemical Solid-State Study of a Series of TTF Radical-Cation Halides with Various Stoichiometries

**Myriam Lamache,* Hubert Menet,[†] and Alec Moradpour[‡]**

*Contribution from the Laboratoire de Chimie Analytique, Université Pierre et Marie Curie, 75005 Paris, France, and the Laboratoire de Physique des Solides, Université Paris-Sud, 91405—Orsay, France.* *Received October 5, 1981*

**Abstract:** The electrochemistry of TTF has been studied in various aqueous media by using carbon paste electrodes. In 1 M acetate, the oxidation of solid TTF proceeds, as in solution, in two one-electron steps, through the successive formation of $TTF^+$ and $TTF^{2+}$ species. But, in chloride and bromide media, the formation of several mixed-valence salts ($(TTF)Cl_{0.7}$, $(TTF)Br_{0.05}$, and $(TTF)Br_{0.7}$) is detected on the current–voltage curves. These studies may provide a new way to investigate the preparative conditions, the compositions and stabilities of various possible solid phases, and the redox behavior of these organic materials.

One-dimensional highly conducting solids, intensively studied over the last decade,[1-4] are presently the subject of renewed interest due to the recent discovery of the existence of superconductivity for some of these organic materials.[5,6] Various molecular

---

[†] Laboratoire de Chimie Analytique.

[‡] Laboratoire de Physique des Solides.

(1) "Chemistry and Physics of One-dimensional metals", Keller, H. J. Ed.; Plenum Press: New York, 1977.

0002-7863/82/1504-4520$01.25/0